Surface & Coatings Technology 381 (2020) 125113

Contents lists available at ScienceDirect

Surface & Coatings Technology

journal homepage: www.elsevier.com/locate/surfcoat

Modifying the surface of a titanium alloy with an electron beam and a-C:H:SiO$_x$ coating deposition to reduce hemolysis in cardiac assist devices

A.S. Grenadyorov[a], A.A. Solovyev[a,*], K.V. Oskomov[a], S.A. Onischenko[a], A.M. Chernyavskiy[b], M.O. Zhulkov[b], V.V. Kaichev[c]

[a] Institute of High Current Electronics, Siberian Branch of the Russian Academy of Sciences, 2/3 Akademichesky ave, Tomsk, 634055, Russia
[b] National Medical Research Center named after E.N. Meshalkin, 15 Rechkunovskaya, Novosibirsk, 630055, Russia
[c] Federal Research Center Boreskov Institute of Catalysis, 5 Lavrentiev Ave, Novosibirsk, 630090, Russia

ARTICLE INFO

Keywords:
Heart failure
Cardiac assist device
Hemolysis
Electron beam treatment
a-C:H:SiO$_x$ coating
Roughness
Friction coefficient

ABSTRACT

The use of implantable mechanical pumps to support stable heart function saves lives to a large number of patients. The priority goal of research in this area is to develop advanced pumps that will ensure minimal injuries and fractures of blood cells. A combined method of modifying the surface of disk pump parts made of titanium alloy VT-6 has been developed to reduce blood hemolysis. The method includes material pretreatment with a high-current low-energy electron beam and plasma-enhanced chemical vapor deposition of a-C:H:SiO$_x$ coating. The effect of such electron beam parameters as the energy density and the number of pulses on the surface morphology, hardness, plasticity index, friction coefficient and wear rate of the titanium alloy was studied. The effect of the 1.6-µm-thick a-C:H:SiO$_x$ coating on the surface morphology, mechanical and tribological properties of VT-6 samples subjected to preliminary electron beam processing was also investigated. Parts of the disk pump were modified according to the proposed technology and pump was tested on the degree of red blood cell destruction. After modifying the surface of pump parts, the destruction of red blood cells did not occur during the 4-h experiment, unlike a similar pump without surface modification. It is shown that the physical properties of the surface are one of the most important factors affecting hemolysis in mechanical pumps to support stable heart function.

1. Introduction

It is known that mortality from cardiovascular diseases is in the first place all over the world, in particular due to acute damage to the heart muscle (myocardial infarction, acute myocarditis, etc.) [1]. In this regard, attempts are being made to use implantable mechanical pumps to support stable heart function (cardiac assist devices) [2–5]. Such pumps have shown good prospects and can be used not only until the normal functioning of the heart is restored, but also as a substitute for heart function for a long time in sick people who donor organ transplant is contraindicated or lack a suitable donor organ [6,7].

A lot of research has been done to create problem-free pump designs such as a roller pump, an impeller pump, and a disc pump [8]. However, roller and impeller devices have limited clinical use due to ongoing operational and pathological difficulties. In disk pumps, liquid pumping occurs as a result of the transfer of rotational energy from the disks due to the friction force in the boundary layers. The main advantage of this type of pump is that the principle used to transfer energy from the pump to the liquid fewer damages the blood cells.

The serious problems of any mechanical pumps to support the work of the heart include: 1) the formation of blood clots on the surfaces of the pump in contact with blood; 2) the destruction of blood cells (erythrocytes) during the operation of the device; 3) wear and release of metal ions/particles resulting in stenosis and restenosis [6,9–11]. In addition, the application of these devices slows down due to difficulties with bleeding, infection, and device failure.

The design optimization of multiple disk pumps was carried out mainly by changing the number of disks and the distance between them [12]. The influence of disk material, its surface quality, and mechanical properties on the destruction of blood cells have not been previously studied. Although it is known that the critical factor determining the effectiveness of any medical device in contact with the human biological environment is the interface between the artificial material and biological environment [13]. In addition to the biomechanical characteristics, the nature of the interaction will be determined by the physical and chemical properties of the material and its surface, as well

* Corresponding author.
E-mail address: andrewsol@mail.ru (A.A. Solovyev).

https://doi.org/10.1016/j.surfcoat.2019.125113
Received 7 August 2019; Received in revised form 4 October 2019; Accepted 27 October 2019
Available online 02 November 2019

Table 1
The chemical composition of titanium alloy VT-6.

Al, %	V, %	Ti, %	Zr, %	Fe, %	O, %	Si, %	C, %	N, %	H, %	Other impurities
5.3–6.8	3.5–5.3	86.45–90.9	to 0.3	to 0.3	to 0.2	to 0.15	to 0.1	to 0.05	to 0.015	to 0.3

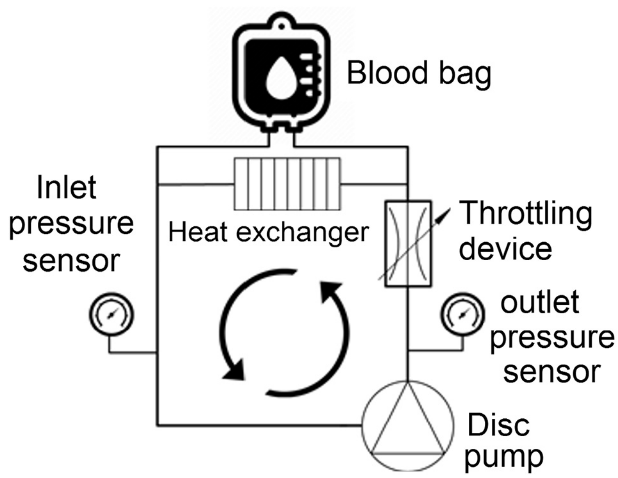

Fig. 1. The diagram of the hemodynamic stand for the study of blood hemolysis.

as their hemocompatibility.

The solution to the above problems can be achieved by modifying the surface of the materials used to manufacture mechanical pumps to support the work of the heart. The surface modification allows changing the morphology and structure of the surface and also contributes to the change of surface properties in a wide range. The most common methods of surface modification include are electron-beam treatment [14,15], as well as the coating deposition with different physical and biomechanical properties [16]. Processing materials with low-energy (up to 40 keV), high-current electron beams (up to 40 J/cm^2) of microsecond duration allows, due to pulsed melting, to dissolve particles of the second phases and, due to ultrafast (10^9 K/s) quenching from a liquid state, to form non-equilibrium structural phase states in thin surface layers [17].

Coatings based on carbon, in particular, diamond-like carbon (DLC), have great prospects for medical applications since they have unique mechanical, tribological, and biomedical properties [18]. Adding silicon or SiO_x phase to the structure of a diamond-like carbon helps reduce inflammatory reactions [19,20], increases biocompatibility with human biological environment [21], reduces the level of restenosis [22], and also helps to reduce blood clots [23,24] and neointimal hyperplasia [23] on stents. At the same time, adhesion strength of a-C:H:SiO_x coatings is significantly higher than that of DLC [25]. This is due to the formation of Si–C bonds that are longer than C–C bonds (the length of Si–C bonds is 1.89 Å, and the length of C–C bonds is 1.54 Å) [26], which ensures good adhesion to a wide range of substrates, while the mechanical and tribological properties remain high [27].

This work is devoted to the study of the effect of surface treatment of titanium alloy VT-6 on the degree of destruction of red blood cells. Erythrocyte destruction was assessed by the release of free hemoglobin. Titanium alloy VT-6 (Ti–6Al–4V)) is among the most common metallic biomaterials [28]. One of the important factors limiting the long-term stability of surgical implants made from this alloy is the risk of metal particles and aluminum ions and, especially, vanadium ions entering adjacent tissues [29]. Therefore, a method of surface modifying of this alloy should not only reduce the degree of destruction of erythrocytes but also minimize the direct contact of the alloy with the human biological environment.

2. Experimental

Combination of two methods for modifying the surface of materials, electron-beam treatment (EBT) and plasma-enhanced chemical vapor deposition (PECVD) of a-C:H:SiO_x coating was used. The structure of the electron gun and its main parameters are described in more detail in Ref. [15]. In the experiments, beams with an energy density of 4 and 6.5 J/cm^2 were used, and the number of pulses was varied from 5 to 15.

The PECVD method and parameters of a-C:H:SiO_x coatings deposition process were described in detail in Refs. [30,31]. Coatings were deposited in a vacuum installation equipped with a plasma generator with heated cathode working in a mixture of argon and polyphenylmethylsiloxane (PPMS) vapor. The base pressure in the chamber was 0.01 Pa. Before coating deposition, the substrates were treated in Ar plasma with a pressure of 0.3 Pa for 6 min. Discharge voltage and current of non-self-contained arc discharge with a heated cathode were 100 V and 11 A, respectively. A filament cathode was heated by the current of 50 A. An external magnetic field with an induction of about 3 G in the substrate region was used to increase the degree of plasma ionization. Bipolar bias voltage with a negative pulse amplitude of 1000 V and a frequency of 100 kHz was applied to the substrate during plasma treatment. The coating was deposited at an Ar pressure of 0.1 Pa, PPMS flow rate of 95 µl/min, discharge voltage of 140 V, discharge current of 6 A and the same value of the magnetic field. During the coating deposition, the negative pulse amplitude of the bipolar bias voltage was reduced to 500 V. Coating deposition rate was 1.8 µm/h.

Titanium alloy plates (composition is shown in Table 1) with a size of $20 \times 20 \times 0.2$ mm^3 were used as substrates.

The µVizo-MET-221 optical microscope was used to study the defects in large surface areas of 0.5×0.5 mm^2. Atomic force microscopy (AFM, Solver P47) was used to study the surface morphology and the surface roughness. AFM data were analyzed using the Gwyddion software. Scanning electron microscopy (SEM, Quanta 2000) was used to obtain images of the surface of the samples. The nanoindentation method (NanoTest 600) was used to measure the hardness and elastic modulus of the obtained samples according to the Oliver-Farr method with a load of 10 mN. The loading rate was 0.54 mN/s. Ten measurements were done on every sample. Pin on the Disc and Oscillating TRIBOtester (TRIBOtechnic, France) was used to measure the friction coefficient and sample wear rate. A ball made of VK-8 alloy with a diameter of 6 mm was used as a counterbody. The disk rotation speed was 25 mm/s, the load was 3 N, and the passed distance was 200 m. The air temperature during the measurement was 25 °C and the relative humidity was 50%. The wear rate was determined by the following formula:

$$V = \frac{2 \cdot \pi \cdot R \cdot A}{F \cdot L}$$

where R is the track radius in micrometers, A is the cross-sectional area of the wear area in µm^2, F is the value of the applied load in N, L is the distance passed by the ball in meters.

The elemental composition of the obtained films was studied by X-ray photoelectron spectroscopy (XPS) using a SPECS Surface Nano Analysis GmbH spectrometer. To record the spectra, monochromatized Al Kα radiation (hν = 1486.74 eV) was used. The relative content of elements in the analysis zone was determined from the integrated intensities of the XPS lines taking into account the photoionization cross-sections of the corresponding terms. Data processing was performed using the CasaXPS software package. The shape of the peaks is

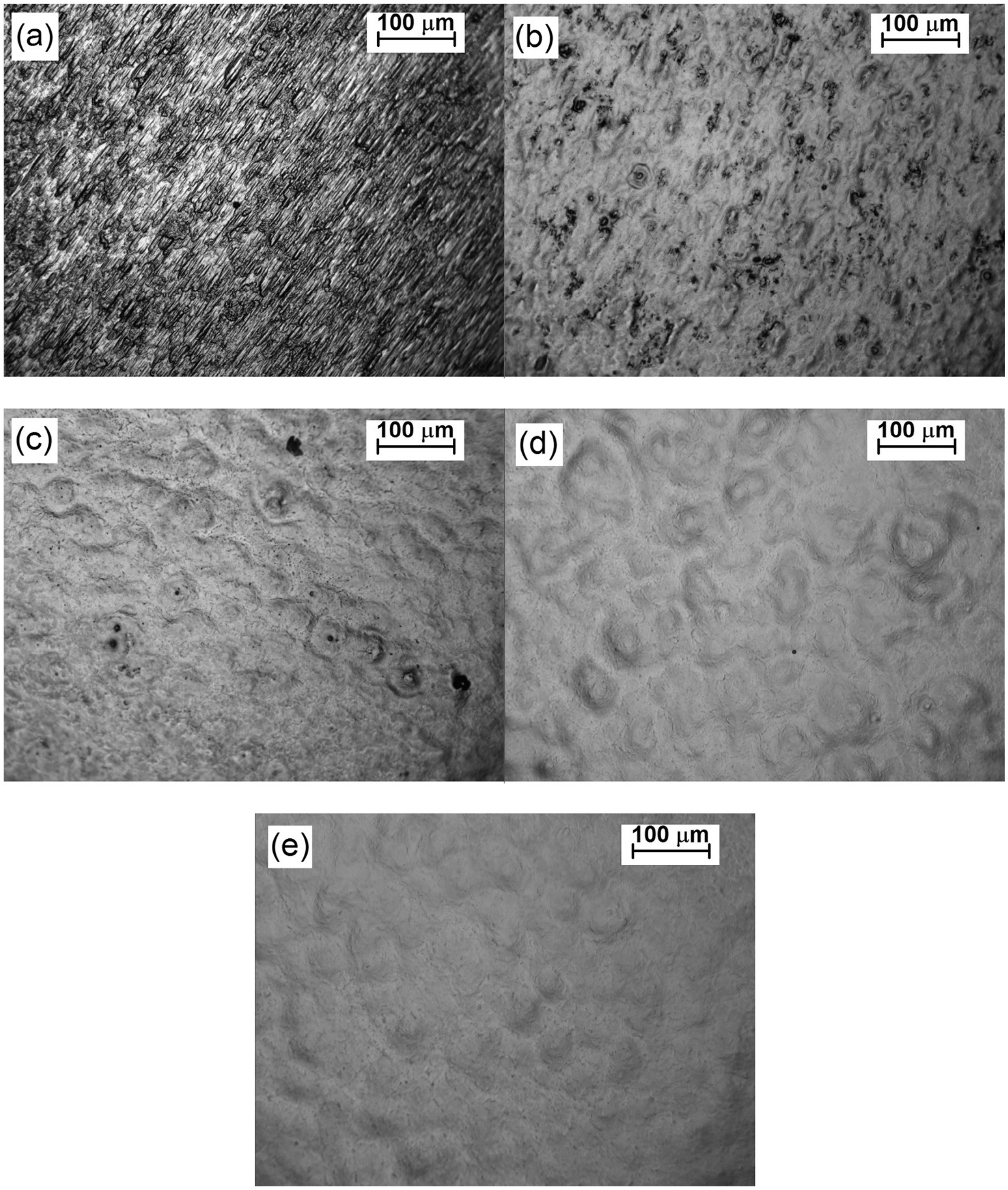

Fig. 2. Images of the titanium alloy VT-6 surface, obtained using optical microscopy: (a) the original surface; (b) after EBT with $E = 4\ J/cm^2$ and $N = 5$; (c) after EBT with $E = 6.5\ J/cm^2$ and $N = 5$; (d) after EBT with $E = 6.5\ J/cm^2$ and $N = 10$; (e) after EBT with $E = 6.5\ J/cm^2$ and $N = 15$.

approximated by the Gauss functions. To remove the surface layer, ion etching with an Ar^+ ion beam with energy of 2. keV for 100 s was used. The Raman spectra were recorded using Centaur U HR spectrometer (Nano Scan Technology, Russia) with 532 nm wavelength. Spectra were recorded with a laser power of 10 mW and within a spectral range of 800–1800 cm^{-1} with a spectral resolution better than 1.5 cm^{-1}.

To measure the degree of destruction of erythrocytes, a hemolysis test was used, which was carried out on a hemodynamic stand simulating the human circulatory system (Fig. 1). A disk pump made of titanium alloy VT-6 was used as a pumping device [32]. The working part of the pump is a package of disks arranged with a fixed gap. Blood pumping occurs as a result of the transfer rotational energy from disks due to friction force in the boundary layers.

Initially, the hemodynamic stand was washed with saline, then filled with a mixture of whole blood and saline at a concentration of 1:1 and a zero blood sample was taken. Then the pump was turned on at a rotational speed of 2850 rev/min, after which blood samples were taken every 30 min. Plasma free hemoglobin level was measured in milligram-percent (1 mg% = 10 mg/l).

3. Results

3.1. Optical microscopy of the titanium alloy

Fig. 2 shows images of the titanium alloy VT-6 surface before and after treatment by an electron beam with different energy density E and number of pulses N. Images were obtained using an optical microscope with the same magnification. Initially, the surface of the titanium alloy has a rough structure composed of microcracks, micro-scratches and cavities (Fig. 2,a). The electron beam treatment leads to the melting of the surface layer with the subsequent smoothing of the surface and the elimination of microcracks and micro-scratches. At an electron beam energy density of $4\ J/m^2$ and $N = 5$ (Fig. 2,b), a large number of defects remain on the surface, although at the same time there are melted areas

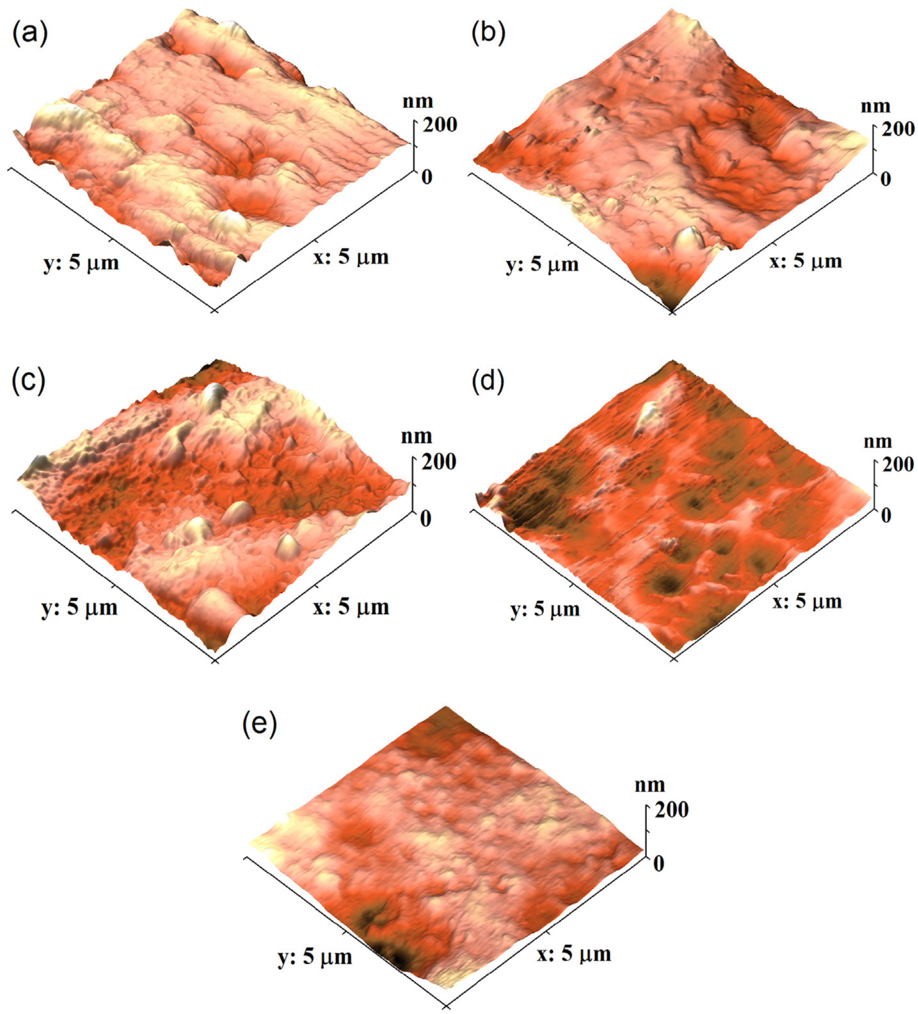

Fig. 3. Surface images of titanium alloy VT-6, obtained by atomic force microscopy: (a) the original surface, (b) after EBT with $E = 4\,\mathrm{J/cm^2}$ and $N = 5$; (c) after EBT with $E = 6.5\,\mathrm{J/cm^2}$ and $N = 5$; (d) after EBT with $E = 6.5\,\mathrm{J/cm^2}$ and $N = 10$; (e) after EBT with $E = 6.5\,\mathrm{J/cm^2}$ and $N = 15$.

Table 2
The surface roughness of the titanium alloy VT-6 samples before and after processing by an electron beam.

Sample according to Fig. 3	R_{mean} (nm)	R_q (nm)	$R_{\max}$ (nm)	R_a (nm)
a	125	22.4	206	16.3
b	79	15.5	147	11.9
c	49.3	13.7	97	11.2
d	23.2	7.8	63	6.2
e	28.6	6.9	54	5.2
Sample d + a-C:H:SiO_x coating	23.4	*7.3*	50.2	5.8

where R_{mean} is the average height of the peaks, R_q is the root-mean-square surface roughness, $R_{\max}$ is the maximum height of the peaks, R_a is the arithmetic mean roughness.

with a smoother surface. As the electron beam energy density increases to $6.5\,\mathrm{J/cm^2}$, the surface smooths significantly, even with $N = 5$ (Fig. 2,c). In this case, a small amount of defects remains on the surface, which can be eliminated by increasing the number of pulses. After EBT with $E = 6.5\,\mathrm{J/cm^2}$ and $N = 10$–15 (Fig. 2d and e) on the surface there are practically no defects such as microcracks and micro-scratches. Only deep dimples are present. Thus, the effect of an electron beam on the surface of a titanium alloy allows one to radically smooth its surface.

3.2. Atomic force microscopy of the titanium alloy

Fig. 3 shows images of the titanium alloy VT-6 surface before and after processing by an electron beam with different energy density and number of pulses, obtained using atomic force microscopy in areas of size $5 \times 5\,\mu\mathrm{m}^2$. Table 2 presents the results of measuring the surface roughness in these areas.

It is seen that an increase in the electron beam energy density and the number of pulses leads to a decrease in the surface roughness. Due to the effect of the electron beam, it is possible to reduce the root-mean-square surface roughness from 22.4 nm (the original surface) to 6.9 nm (after electron-beam surface treatment with $E = 6.5\,\mathrm{J/cm^2}$ and $N = 15$).

3.3. Scanning electron microscopy of the titanium alloy

Fig. 4 shows images of the surface of the titanium alloy VT-6 before and after processing by an electron beam with different energy density and number of pulses, obtained using scanning electron microscopy with the same magnification. On the original surface (Fig. 4, a) one can see micro-scratches formed in the process of titanium sheets manufacturing. When a sample is exposed to a beam with an energy density of $4\,\mathrm{J/cm^2}$ (Fig. 4,b), it can be seen that the surface melts at the places where the maximum electric field is generated, i.e. on microstrips and microcracks. An increase in the energy density of the beam and the number of pulses leads to the melting of the entire surface of the

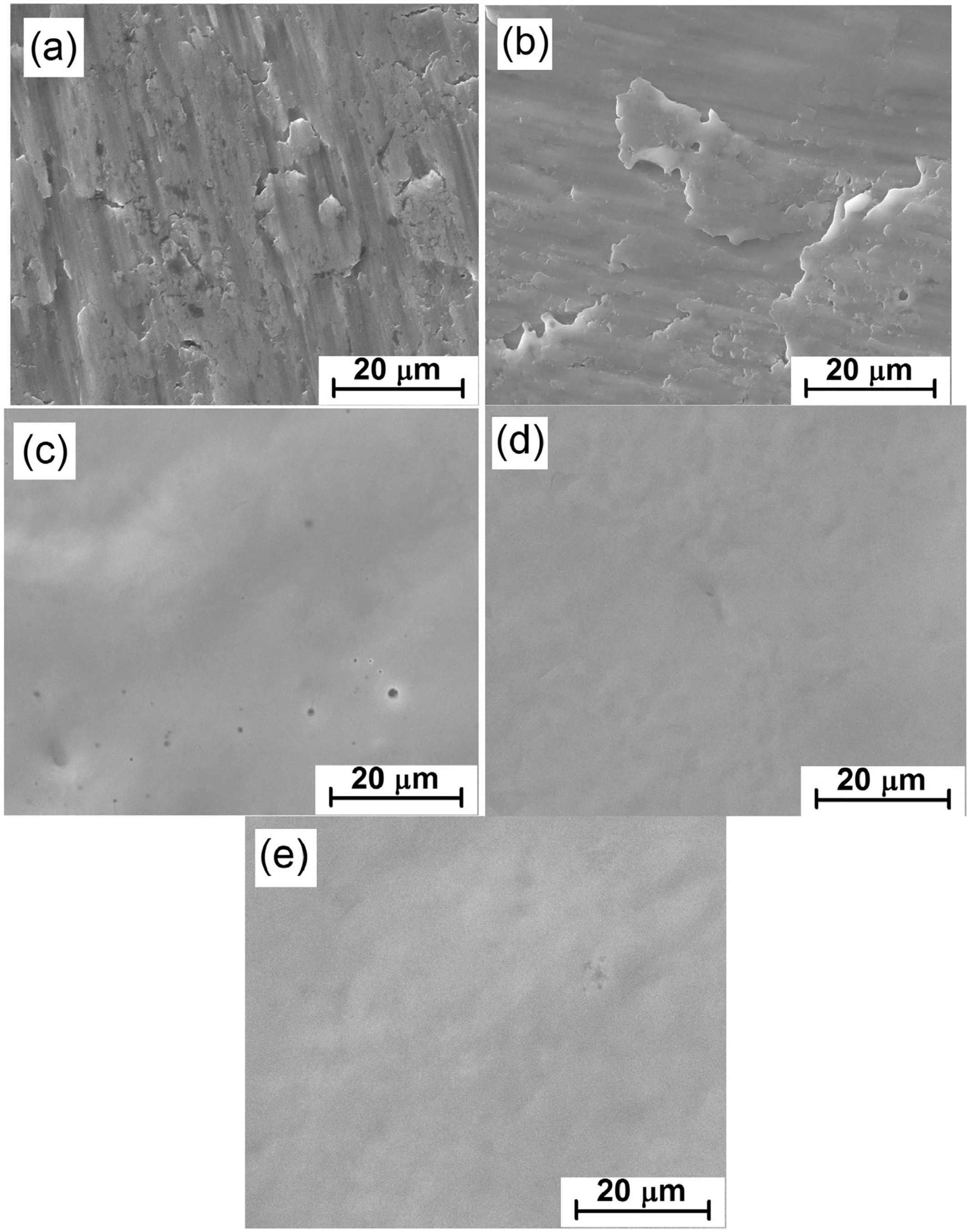

Fig. 4. Images of the titanium alloy VT-6 surface, obtained using scanning electron microscopy: (a) the original surface, (b) after EBT with E = 4 J/cm^2 and N = 5; (c) after EBT with E = 6.5 J/cm^2 and N = 5; (d) after EBT with E = 6.5 J/cm^2 and N = 10; (e) after EBT with E = 6.5 J/cm^2 and N = 15.

sample. The best result in terms of surface smoothing and minimizing the number of defects on it is observed after electron-beam treatment with E = 6.5 J/cm^2 and N = 10 (Fig. 4,d). An increase in the electron beam energy density or the number of pulses (more than 10) does not lead to a more pronounced smoothing of the sample surface (Fig. 4,e), while the probability of crater formation at the locations of impurities increases.

3.4. Mechanical characteristics and tribological tests of the titanium alloy

Fig. 5 shows the dependence of hardness and plasticity index H/E of several samples of titanium alloy VT-6 on the treatment mode by an electron beam. It can be noted that an increase in the energy density and the number of pulses leads to an increase in hardness from 2.12 to 3.01 GPa and plasticity index H/E from 0.03 to 0.05.

The increase of hardness of surface layer is explained by its quenching from the liquid state. The increased hardness in this layer is due to strain hardening under the action of quasi-static stresses formed at the stage of cooling after the completion of crystallization [33].

Fig. 6 shows the dependence of the friction coefficient on time (a), hardness and wear rate (b) for a titanium alloy VT-6 samples without treatment (S1) and after EBT with E = 6.5 J/cm^2 and N = 10 (S2). It can be noted that the friction coefficient of the titanium alloy after treatment with an electron beam decreases insignificantly (average value decreases from 0.68 to 0.64). The wear rate of the sample decreases slightly from 9.4×10^{-4} to 6.8×10^{-4} mm^3/N·m. This is

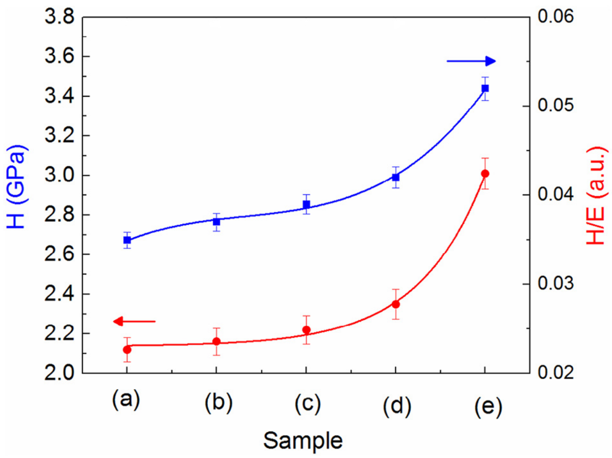

Fig. 5. Dependence of hardness and plasticity index of titanium alloy VT-6 on the parameters of electron-beam treatment: (a) the original surface, (b) after EBT with $E = 4\ \mathrm{J/cm^2}$ and $N = 5$; (c) after EBT with $E = 6.5\ \mathrm{J/cm^2}$ and $N = 5$; (d) after EBT with $E = 6.5\ \mathrm{J/cm^2}$ and $N = 10$; (e) after EBT with $E = 6.5\ \mathrm{J/cm^2}$ and $N = 15$.

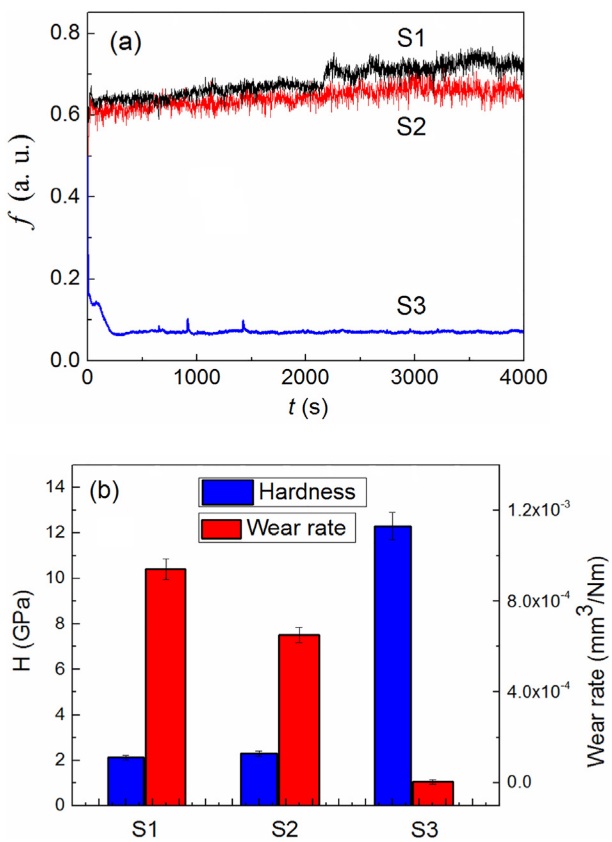

Fig. 6. Dependence of the friction coefficient f on time (a), hardness and wear rate values (b) for a titanium alloy VT-6 samples without treatment (S1); after EBT with $E = 6.5\ \mathrm{J/cm^2}$ and $N = 10$ (S2); after EBT and a-C:H:SiO_x coating deposition (S3).

apparently due to an increase in the surface hardness of the sample as shown in Fig. 5. Thus, EBT leads not only to an increase in the hardness of the sample surface but also to an increase in its wear resistance.

3.5. a-C:H:SiOx coating deposition and test

Fig. 7 shows the SEM and AFM surface images of the 1.6-μm-thick a-C:H:SiO_x coating deposited on a sample whose surface was treated with an electron beam with $E = 6.5\ \mathrm{J/cm^2}$ and $N = 10$. From these images and Table 2, it can be seen that the surface of the sample after the coating deposition retains low roughness values and even becomes slightly smoother.

Fig. 8 presents the results of the a-C:H:SiO_x coating study by X-ray photoelectron spectroscopy. Fig. 8,a illustrates the full XPS spectrum of coating taken in the energy range from 0 to 1100 eV. It can be noted that the following main bands are distinguished in the obtained coating: in the region of 36 eV – W *4f*, 100 eV – Si *2p*, 152 eV – Si *2s*, 250 eV – W *3d*, 284 eV – C *1s*, 400 eV – N *1s*, 532 eV – O *1s* and 978 eV – O (*KLL*). The presence of W and N lines in the spectrum can be explained by the evaporation of a heated tungsten cathode and the presence of a residual atmosphere in the chamber, respectively. According to the XPS results, the elemental composition of a-C:H:SiO_x coating: C – 55 at.%, Si – 13 at. %, O – 25 at. %, N – 4 at.%, W - 3 at.%. Although the H concentration could not be measured by XPS, the presence of H in the coating is confirmed by the presence of photoluminescence background in the Raman spectra of a-C:H:SiO_x coatings obtained earlier [31].

Fig. 8,b-d shows Si *2p*, C *1s* and O *1s* bands with dividing into Gaussian using the Origin program. All bands are not symmetrical due to the presence of more than one chemical state within these bands.

Si *2p* band corresponds to the energy range 98.5–106 eV with a center in the 102 eV. This band is divided into 4 peaks. The first peak at energy of 98.9 eV corresponds to Si–Si bonds, the second peak at 100.3 eV, is consistent with silicon carbide bonds, and third peak at energy of 102.1 eV, most likely arises from the presence of chemical bonds where the ratio of Si to oxygen is increased which is consistent with the presence of polymeric siloxane structures, (–Si(R_1)(R_2)–O–)$_n$ [34]. Where R_1 and R_2 represent aliphatic and/or aromatic organic structures. The fourth peak located at around 105 eV corresponds to SiO_2 [35]. Thus, the Si *2p* band revealed that the polymeric siloxane structures predominantly exist with a minor portion of Si–Si, Si–C and SiO_2 bonds. Si *2s* peak at energy of 152 eV represents Si–O bonding.

The C *1s* peak for a-C:H:SiO_x coating can be deconvoluted into three peaks as shown in Fig. 8,c. It means that three different types of chemical bonds are found for carbon in the deposited coating. A peak at 284.3 eV is characteristic of the C–C bond, a peak at 286.2 eV is indicative of the C–O bond and a peak at 287.9 eV belongs to the carbon-oxygen bond (C═O) [35–37].

The binding energy for the O *1s* peak is found at 532 eV. This band is characterized by two peaks belonging to the C═O and C–O bond and located at 530.1 eV and 531.9 eV [35]. The XPS results mean that polymeric siloxane structures, C–C and C–O bonds dominantly exist in the coating, while Si–C and C═O bonds are less presented.

Fig. 9 shows the Raman spectrum of a-C:H:SiO_x coating on titanium alloy VT-6. It represents a broad asymmetric peak in the wavenumber range of 1000–1700 $\mathrm{cm^{-1}}$, typical of carbon-based films. This spectrum was deconvoluted into two Gaussian peaks: the G peak and D peak by curve fitting. The positions of these peaks in the spectrum, the full width at half the maxima (FWHM) of the G peak and the I_D/I_G intensity ratio are the most important parameters for understanding the properties of carbon films, such as the ratio of sp^2 to sp^3 hybridized carbon atoms and the stress level in the film [38].

For the obtained a-C:H:SiO_x coating, the D and G peaks are located at the wavenumbers of 1330 and 1494 $\mathrm{cm^{-1}}$, respectively. The I_D/I_G ratio is 0.83, and the FWHM of the G peak is 180 $\mathrm{cm^{-1}}$. Similar parameters of the D and G peaks were observed by Batory et al. [39] for a-C:H:SiO_x coatings obtained by the RF PECVD method from gas mixtures composed of CH_4 and hexamethylodisiloxane.

After deposition of a-C:H:SiO_x coating on a sample of titanium alloy VT-6, processed by an electron beam with $E = 6.5\ \mathrm{J/cm^2}$ and $N = 10$, the sample hardness increases by a factor of 5 from 2.3 to 12.3 GPa (Fig. 6,b). Accordingly, the plasticity index H/E increases from 0.042 to 0.107 and the resistance to plastic deformation H^3/E^2 increases from 4.1 to 144.3 MPa.

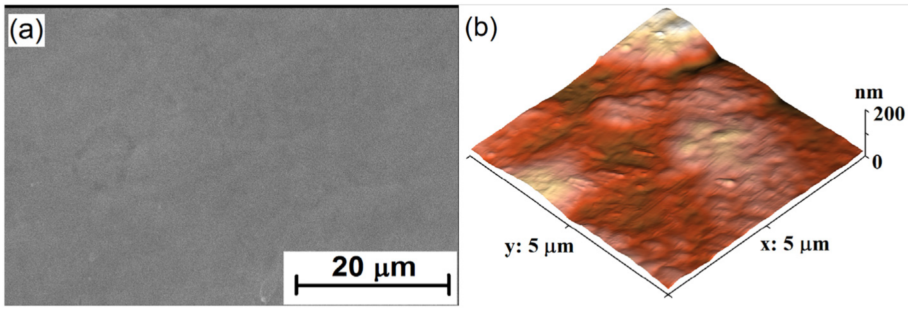

Fig. 7. Surface SEM (a) and AFM (b) images of the a-C:H:SiO_x coating deposited on a titanium alloy VT-6, pre-treated by an electron beam with a with E = 6.5 J/cm^2 and N = 10.

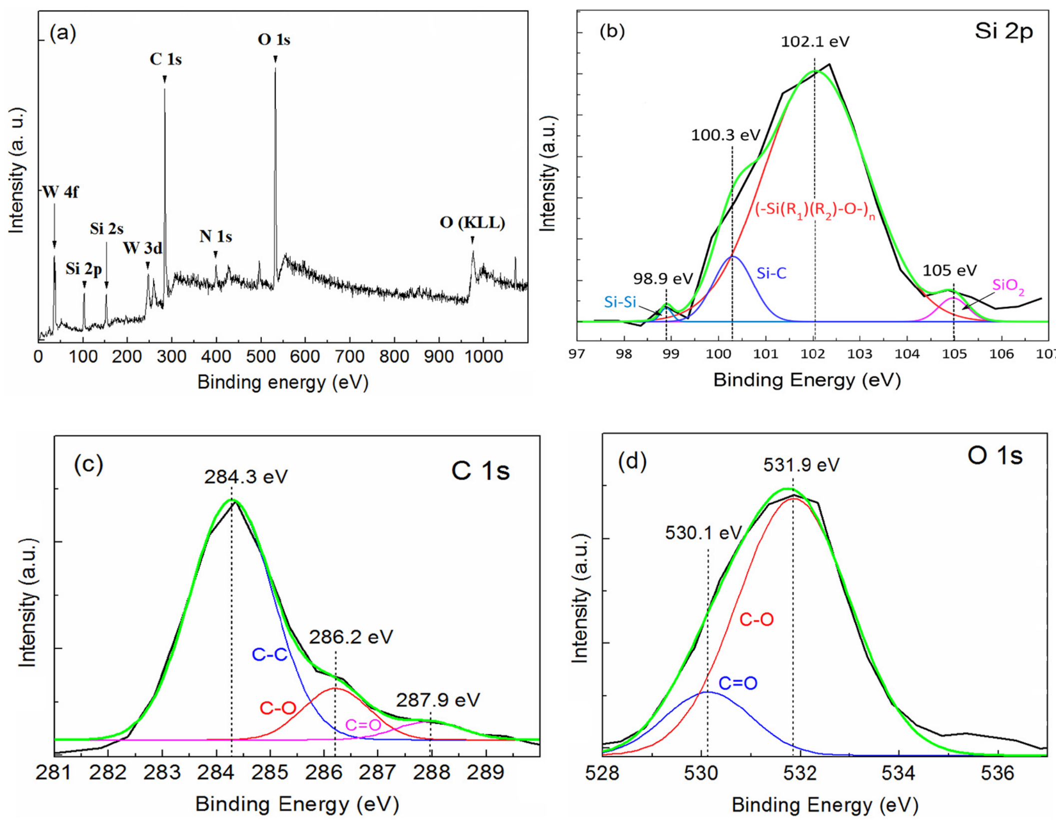

Fig. 8. XPS spectra a-C:H:SiO_x coating: a – total spectrum, b – Si *2p* band, c – C *1s* band, d – O *1s* band.

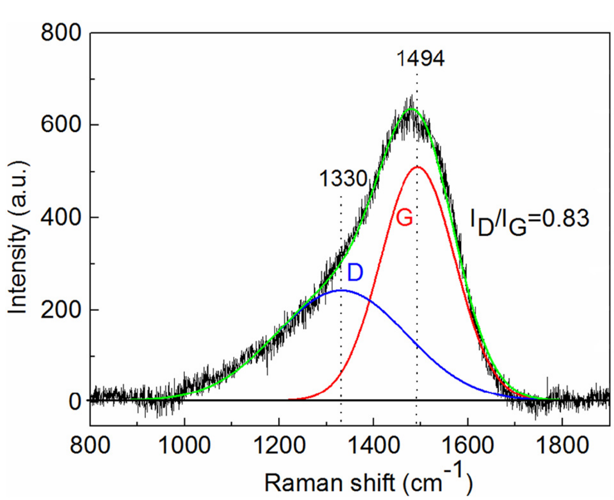

Fig. 9. Raman spectrum of a-C:H:SiO_x coating on titanium alloy VT-6.

In addition to improving the mechanical characteristics of the surface, the a-C:H:SiO_x coating deposition leads to a decrease in the friction coefficient to less than 0.1 (Fig. 6,a). The wear rate of the coated sample is reduced by two orders, from 6.5 × 10^{-4} to 4 × 10^{-6} mm^3/N·m (Fig. 6,b).

3.6. Disk pump testing on the degree of red blood cells destruction

For testing a disk pump on the degree of red blood cell destruction, the surface of its parts was modified using an electron beam (E = 6.5 J/cm^2 and N = 10) and deposition of 1.5-μm-thick a-C:H:SiO_x coating. The photo of modified pump parts is shown in Fig. 10.

Fig. 11 shows the dependence of the level of free hemoglobin in the blood on the operation time for a disk pump before modifying the surface of its parts (1) and after modifying its parts surface with an electron beam treatment and a-C:H:SiO_x coating deposition (2).

It is seen that over time in the pump with the unmodified surface of the parts there is a practically continuous increase in the level of free hemoglobin. Although after 4 h of work, the level of free hemoglobin

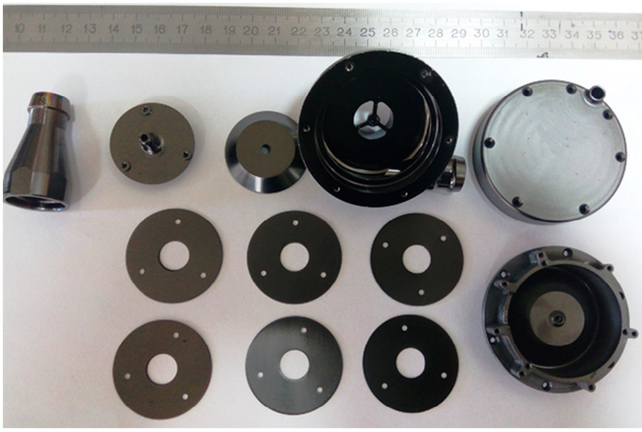

Fig. 10. Photo of disk pump parts after electron beam processing and a-C:H:SiO$_x$ coating deposition.

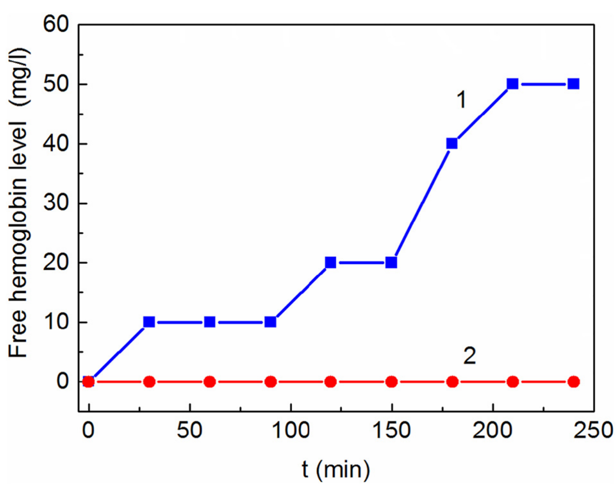

Fig. 11. Dependence of the level of free hemoglobin in the blood on the operation time for a disk pump before modifying the surface of its parts (1) and after modifying of its parts surface with an electron beam treatment and a-C:H:SiO$_x$ coating deposition (2).

does not exceed the permissible level (100 mg/l). After modifying the surface of the pump parts by an electron beam and a-C:H:SiO$_x$ coating deposition, erythrocyte destruction did not occur during the 4-h experiment.

4. Discussion

Although red blood cells easily deform and elongate passing through small capillaries, they could be mechanically damaged at extreme conditions. Mechanical hemolysis is a release of hemoglobin into plasma due to the breaking up of cell membrane as consequence of the movement of blood through the mechanical pumps [40]. Erythrocytes experience high shear forces when passing through narrow gaps and openings in the pump. The erythrocytes passing through the areas remote from the pump parts move at higher speeds than the erythrocytes that are in contact with the surface of the parts. This difference in the speed with which red blood cells pass by each other leads to a high shear force. When the shear force exceeds the critical level, the erythrocyte membranes rupture, resulting in hemolysis [41]. However, there are a number of other factors that may be responsible for erythrocyte damage: (a) interaction of erythrocytes with solid surfaces, (b) centrifugal force, (c) cell-cell interaction, and (d) viscous heating [42,43].

A drastic decrease in the level of free hemoglobin in the blood we can explain mainly by the significant decrease in surface roughness of modified pump parts. This is primarily due to the consequence of electron beam treatment. A qualitative change in the surface after EBT can be seen even with the naked eye. The small roughness of the parts leads to viscous friction with the character of fluid movement in the gap close to laminar and low shear stresses. The effect of the a-C:H:SiO$_x$ coating on hemolysis remains open to question. However, the coating has its own equally important functions. Coating leads to a significant increase in the hardness and wear resistance of the pump parts surface, which is always important for devices with moving parts. Increased wear resistance will reduce the probability of metal microparticles incoming the human body. In addition, the reduction of the friction coefficient should reduce the heating of the pump when it is working. An important effect of a-C:H:SiO$_x$ coating is the creation of a physical barrier between the atoms/ions of aluminum and vanadium in the VT-6 alloy and human blood.

Such a synergistic effect from the combined surface treatment we observed in the study of pulse dielectric gaps with different electrode materials [44]. It has been shown that electron beam treatment of titanium foil can increase the short-pulse electric strength of the vacuum gap between Ti electrodes from 0.9 to 1.5 MV/cm. Initially, the surface of the titanium electrode has a lot of microcracks formed during the manufacturing process of titanium foil. On the sharp edges of the microcracks, the electric field strength increases and, accordingly, the breakdown occurs at a lower applied voltage. Treatment the electrodes using a low-energy, high-current electron beam eliminates microcracks by melting the surface layers of the electrode material. R_q surface roughness is significantly reduced compared with untreated electrodes from 93 to 15 nm. The deposition of 2.9-µm-thick a-C:H:SiO$_x$ coating on the electron-beam-treated electrodes leads to a decrease in the R_q surface roughness of up to 7 nm and an increase in dielectric strength to 1.9 MV/cm.

5. Conclusion

In this study, a novel combined method of modifying the surface for medical devices to reduce blood hemolysis has been developed. The method includes titanium alloy pretreatment with a high-current low-energy electron beam with an energy density of 6.5 J/cm^2 and number of pulses N = 10–15 and subsequent plasma-enhanced chemical vapor deposition of 1.6-µm-thick a-C:H:SiO$_x$ coating. Pulsed electron beam treatment leads to significant decrease of the root-mean-square surface roughness (from 22.4 nm to 6.9 nm) and increases of surface layer hardness (from 2.12 to 3.01 GPa) due to quenching from the liquid state. Deposition of a-C:H:SiO$_x$ coating on the pretreated by electron beam sample increases its hardness from 2.3 to 12.3 GPa, the plasticity index H/E increases from 0.042 to 0.107 and the resistance to plastic deformation H^3/E^2 increases from 4.1 to 144.3 MPa. In addition, the a-C:H:SiOx coating deposition leads to a decrease in the friction coefficient to less than 0.1 and decrease in wear rate from 6.5×10^{-4} to 4×10^{-6} mm^3/N·m. Modifying the parts of a disk pump for mechanical support of the heart with this method has allowed to radically reduce the shear stresses in the pumped blood and the damage of red blood cells. This solves the problem of hemolysis, which is one of the fundamental problems limiting device success and bring us closer to creating the ideal device that is 100% physiological and safe for the patient. In the next experiments, it is planned to study the process of the thrombosis on surface of titanium parts with a-C:H:SiO$_x$ coating, which is another fundamental problem of these medical devices. Also, animal experiments are planned to perform *in vivo*.

Acknowledgment

This work was supported by the grant of the Russian Science Foundation, project No. 19-19-00186. The authors are thankful to Tomsk Regional Center for Collective Use of the TSC SB RAS for the provided NanoTest 600 nanoindentator and AFM Solver P47 atomic force microscope. The authors are also grateful to the researcher of the laboratory of plasma emission electronics of the Institute of High Current Electronics SB RAS Krysina O.V. for assistance in conducting optical microscopy of the sample surface and tribological tests.

References

[1] A.J. Lenneman, E.J. Birks, Treatment strategies for myocardial recovery in heart failure, Curr. Treat. Options Cardiovasc. Med. 16 (3) (2014) 287.
[2] S.V. Selishchev, D.V. Telyshev, Optimisation of the sputnik-VAD design, Int. J. Artif. Organs 39 (8) (2016) 407–414.
[3] D.P. Mulloy, C.M. Bhamidipati, M.L. Stone, G. Ailawadi, I.L. Kron, J.A. Kern, Orthotopic heart transplant versus left ventricular assist device: a national comparison of cost and survival, J. Thorac. Cardiovasc. Surg. 145 (2) (2013) 566–573.
[4] D.S. Petukhov, S.V. Selishchev, D.V. Telyshev, Development of left ventricular assist devices as the most effective acute heart failure therapy, Biomed. Eng. 48 (6) (2015) 328–330.
[5] C.S. Jhun, R. Newcwanger, J. Cysyk, B. Lukic, W. Weiss, G. Rosenberg, Tesla-based blood pump and its applications, J. Med. Dev. 7 (4) (2013) 0409171–0409172.
[6] G.P. Itkin, S.Yu Shemakin, E.G. Shokhina, V.I. Burtsev, P.V. Avramov, E.A. Volkova, D.V. Evljukhin, N.P. Shmerko, V.A. Mal'gichev, The first domestic implantable axial flow pump: results of experimental studies in calves, Russ. J. Transplantology Artif. Organs 15 (3) (2013) 49–58.
[7] S.S. Shreenivas, J.E. Rame, M. Jessup, Mechanical circulatory support as a bridge to transplant or for destination therapy, Curr. Heart Fail. Rep. 7 (2010) 159–166.
[8] G.E. Miller, B.D. Etter, J.M. Dorsi, A multiple disk centrifugal pump as a blood flow device, IEEE Trans. Biomed. Eng. 37 (2) (1990) 157–163.
[9] R. Sansone, B. Stanske, S. Keymel, D. Schuler, P. Horn, D. Saeed, U. Boeken, R. Westenfeld, A. Lichtenberg, M. Kelm, C. Heiss, Macrovascular and microvascular function after implantation of left ventricular assist devices in end-stage heart failure: role of microparticles, J. Heart Lung Transplant. 34 (7) (2015) 921–932.
[10] D. Sakota, R. Sakamoto, H. Sobajima, N. Yokoyama, S. Waguri, K. Ohuchi, S. Takatani, Mechanical damage of red blood cells by rotary blood pumps: selective destruction of aged red blood cells and subhemolytic trauma, Artif. Organs 32 (2008) 785–791.
[11] C. Heilmann, U. Geisen, C. Benk, M. Berchtold-Herz, G. Trummer, C. Schlensak, B. Zieger, F. Beyersdorf, Haemolysis in patients with ventricular assist devices: major differences between systems, Eur. J. Cardiothorac. Surg. 36 (3) (2009) 580–584.
[12] G.E. Miller, R. Fink, Analysis of optimal design configurations for a multiple disk centrifugal blood pump, Artif. Organs 23 (6) (1999) 559–565.
[13] J.V. Nepola, External fixation, in: C.A. Rockwood, D.P. Green, R.W. Bucholz, J.D. Heckman (Eds.), Rockwood and Green's Fractures in Adults, vol. 1, Lippincott-Raven Publishers, Philadelphia, 1996, pp. 229–304.
[14] V.P. Rotshtein, D.I. Proskurovsky, G.E. Ozur, YuF. Ivanov, A.B. Markov, Surface modification and alloying of metallic materials with low-energy high-current electron beams, Surf. Coat. Technol. 180–181 (2004) 377–381.
[15] G.E. Ozur, D.I. Proskurovsky, V.P. Rotshtein, A.B. Markov, Production and application of low-energy high-current electron beams, Laser Part. Beams 21 (2) (2003) 157–174.
[16] I.Sh Trakhtenberg, A.P. Rubshtein, E.B. Makarova, A.B. Vladimirov, V.A. Yugov, K. Uemura, Adhesion and metabolic processes of marrow cells on titanium surface with $CN_{0.25}$ film, Diam. Relat. Mater. 17 (2008) 888–891.
[17] D.I. Proskurovsky, V.P. Rotshtein, G.E. Ozur, A.B. Markov, D.S. Nazarov, M.A. Shulov, YuF. Ivanov, R.G. Buchheit, Pulsed electron-beam technology for surface modification of metallic materials, J. Vac. Sci. Technol. A 16 (4) (1998) 2480–2488.
[18] T.T. Liao, T.F. Zhang, S.S. Li, Q.Y. Deng, B.J. Wu, Y.Z. Zhang, Y.J. Zhou, Y.B. Guo, Y.X. Leng, N. Huang, Biological responses of diamond-like carbon (DLC) films with different structures in biomedical application, Mater. Sci. Eng. C 69 (2016) 751–759.
[19] M. Mohanty, T.V. Anilkumar, P.V. Mohanan, C.V. Muraleedharan, G.S. Bhuvaneshwar, F. Derangere, Y. Sampeur, R. Suryanarayanan, Long term tissue response to titanium coated with diamond like carbon, Biomol. Eng. 19 (2–6) (2002) 125–128.
[20] I. De Scheerder, M. Szilard, H. Yanming, X.B. Ping, E. Verbeken, D. Neerinck, E. Demeyere, W. Coppens, F. Van de Werf, Evaluation of the biocompatibility of two new diamond-like stent coatings (Dylyn) in a porcine coronary stent model, J. Invasive Cardiol. 12 (8) (2000) 389–394.
[21] C. Donnet, A. Erdemir, Tribology of Diamond-Like Carbon Films: Fundamentals and Applications, Springer Science and Business Media, 2008.
[22] Y. Yang, Linköping University Medical Dissertation. No 539, Sweden, 91-7219-084-1, 1997 Linköping.
[23] S. Meskinis, A. Tamuleviciene, Structure, properties and applications of diamond like nanocomposite (SiO_x containing DLC) films: a review, Mater. Sci. 17 (4) (2011) 358–370.
[24] D. Antoniucci, A. Bortarelli, R. Valenti, P. Montorsi, G.M. Santoro, F. Fabbiocchi, L. Bolognese, A. Loaldi, M. Trapani, D. Trabattoni, G. Moschi, S. Galli, Clinical and angiographic outcome after coronary arterial stenting with carbostent, Am. J. Cardiol. 85 (7) (2000) 821–825.
[25] N. Kumar, S.A. Barve, S.S. Chopade, R. Kar, N. Chand, S. Dash, A.K. Tyagi, D.S. Patil, Scratch resistance and tribological properties of SiO_x incorporated diamond-like carbon films deposited by r.f. plasma assisted chemical vapor deposition, Tribol. Int. 84 (2015) 124–131.
[26] K. Koshigan, F. Mangolini, J.B. McClimon, B. Vacher, S. Bec, R.W. Carpick, J. Fontaine, Understanding the hydrogen and oxygen gas pressure dependence of the tribological properties of silicon oxide-doped hydrogenated amorphous carbon coatings, Carbon 93 (2015) 851–860.
[27] D. Batory, A. Jedrzejczak, W. Szymanski, P. Niedzielski, M. Fijalkowski, P. Louda, I. Kotela, M. Hromadka, J. Musil, Mechanical characterization of a-C:H:SiO_x coatings synthesized using radio-frequency plasma-assisted chemical vapor deposition method, Thin Solid Films 590 (2015) 299–305.
[28] M. Niinomi, Recent metallic materials for biomedical applications, Metall. Mater. Trans. A 33A (3) (2002) 447–486.
[29] S.G. Steineman, Corrosion of surgical implants—in vivo and in vitro tests, in: G.D. Winter, J.L. Leroy, K. de Goot (Eds.), Evaluation of Biomaterials, John Wiley & Sons, Chichester, 1980, pp. 1–34.
[30] A.S. Grenadyorov, A.A. Solovyev, K.V. Oskomov, O.A. Yaroslavtseva, Mechanical and tribological characteristics of a-C:H:SiO_x films formed by PACVD on titanium alloy VT1-0, IOP Conf. Ser. Mater. Sci. Eng. 511 (2019) 012019.
[31] A.S. Grenadyorov, A.A. Solovyev, K.V. Oskomov, V.S. Sypchenko, Influence of deposition conditions on mechanical properties of a-C:H:SiO_x films prepared by plasma-assisted chemical vapor deposition method, Surf. Coat. Technol. 349 (2018) 547–555.
[32] A.E. Medvedev, V.M. Fomin, A.M. Chernyavskiy, YuM. Prikhodko, M.O. Zhulkov, A.M. Golovin, Implanted system of mechanical support of the disk-based heart pump viscous friction, AIP Conf. Proc. 2027 (2018) 030149.
[33] D.I. Proskurovsky, V.P. Rotshtein, G.E. Ozur, YuF. Ivanov, A.B. Markov, Physical foundations for surface treatment of materials with low energy, high current electron beams, Surf. Coat. Technol. 125 (2000) 49–56.
[34] L.K. Randeniya, A. Bendavid, P.J. Martin, M.S. Amin, E.W. Preston, Molecular structure of SiO_x-incorporated diamond-like carbon films; evidence for phase segregation, Diam. Relat. Mater. 18 (2009) 1167–1173.
[35] S.A. Barve, S.S. Chopade, R. Kar, N. Chand, M.N. Deo, A. Biswas, N.N. Patel, G.M. Rao, D.S. Patil, S. Sinha, SiO_x containing diamond like carbon coatings: effect of substrate bias during deposition, Diam. Relat. Mater. 71 (2017) 63–72.
[36] W.J. Yang, T. Sekino, K.B. Shim, K. Niihara, K.H. Auh, Microstructure and tribological properties of SiO_x/DLC films grown by PECVD, Surf. Coat. Technol. 194 (2005) 128–135.
[37] K. Aumaille, C. Vallée, A. Granier, A. Goullet, F. Gaboriau, G. Turban, A comparative study of oxygen/organosilicon plasmas and thin $SiO_xC_yH_z$ films deposited in a helicon reactor, Thin Solid Films 359 (2000) 188–196.
[38] I. Bertóti, A. Tóth, M. Mohai, J. Szépvölgyi, Chemical structure and mechanical properties of Si-containing a-C:H and a-C thin films and their Cr- and W-containing derivatives, Surf. Coat. Technol. 206 (2011) 630–639.
[39] D. Batory, A. Jedrzejczak, W. Kaczorowski, L. Kolodziejczyk, B. Burnat, The effect of Si incorporation on the corrosion resistance of a-C:H:SiO_x coatings, Diam. Relat. Mater. 67 (2016) 1–7.
[40] S.S. Lee, K.H. Ahn, S.J. Lee, K. Sun, P.T. Goedhart, M.R. Hardeman, Shear induced damage of red blood cells monitored by the decrease of their deformability, Korea Aust. Rheol. J. 16 (3) (2004) 141–146.
[41] O.K. Baskurt, Red blood cell mechanical stability, Engineering 5 (2012) 8–10.
[42] L.B. Leverett, J.D. Hellums, C.P. Alfrey, E.C. Lynch, Red blood cell damage by shear stress, Biophys. J. 12 (3) (1972) 257–273.
[43] S. Deutsch, J.M. Tarbell, K.B. Manning, G. Rosenberg, A.A. Fontaine, Experimental fluid mechanics of pulsatile artificial blood pumps, Annu. Rev. Fluid Mech. 38 (1) (2006) 65–86.
[44] S.A. Onischenko, A.S. Grenadyorov, K.V. Oskomov, E.V. Nefedtsev, A.V. Batrakov, Short pulse dielectric strength of vacuum gaps with different electrode materials, Proceedings of international symposium on discharges and electrical insulation in vacuum, ISDEIV, V. 2016, 2016, https://doi.org/10.1109/DEIV.2016.7748676 Article number 7748676.